

Apparent Horizon Formation and Hoop Conjecture in Non-axisymmetric Spaces

Takeshi Chiba*

Yukawa Institute for Theoretical Physics, Kyoto University, Kyoto 606-01, Japan

(January 13, 2019)

Abstract

We investigate the validity of Thorne’s hoop conjecture in non-axisymmetric spacetimes by examining the formation of apparent horizons numerically. If spaces have a discrete symmetry about one axis, we can specify the boundary conditions to determine an apparent horizon even in non-axisymmetric spaces. We implement, for the first time, the “hoop finder” in non-axisymmetric spaces with a discrete symmetry. We construct asymptotically flat vacuum solutions at a moment of time symmetry. Two cases are examined: black holes distributed on a ring, and black holes on a spherical surface. It turns out that calculating \mathcal{C} is reduced to solving an ordinary differential equation. We find that even in non-axisymmetric spaces the existence or nonexistence of an apparent horizon is consistent with the inequality: $\mathcal{C} \lesssim 4\pi M$.

PACS numbers: 04.20.Dw; 04.25.Dm; 04.70.Bw; 97.60.Lf

Typeset using REVTeX

*Current address: Department of Physics, University of Tokyo, Tokyo 113-0033, Japan

I. INTRODUCTION

In 1972, Kip Thorne proposed the hoop conjecture [1]; *horizons form when and only when a mass M gets compacted into a region whose circumference in every direction is $\mathcal{C} \lesssim 4\pi M$* . However, it took nearly a decade until the studies appeared which directly address the conjecture. This may be because of the vagueness of the statement, i.e., the circumference \mathcal{C} of the horizon and the mass M of a body are ambiguously defined.

For axisymmetric bodies, the definition of \mathcal{C} is rather simple as either the minimum equatorial circumference or the minimum polar circumference [2,3]. Hence there exist a lot of works both by numerical and by analytical approaches addressing the hoop conjecture in the axisymmetric system [2,4–6].

For non-axisymmetric bodies, on the other hand, we didn't have any satisfactory definition of \mathcal{C} until we proposed a definition using closed geodesics [6]. In this paper we demonstrate how to calculate \mathcal{C} in numerically generated spacetime without axisymmetry but with a discrete symmetry and assess the validity of the hoop conjecture. We study the formation of apparent horizons because apparent horizons can be identified locally and provide the practical definition of a black hole. It is important to emphasize here that event horizons may clothe the singularities even if apparent horizons do not appear on the spatial slices considered. The existence of an apparent horizon is a sufficient condition for the formation of an event horizon [7].

Unfortunately there exists an obstacle to study the formation of apparent horizons numerically because we do not have an efficient and robust method to find apparent horizons in general non-axisymmetric spaces, although there has been recent progress [8–11]. This is an important aspect because we are interested in the existence or nonexistence of an apparent horizon. On the other hand, if we allow spaces to have a discrete symmetry (but not continuous one), we can solve the equation for the surface of an apparent horizon, which is generally a nonlinear elliptic equation, as a boundary value problem [10]. Then the numerical treatment of the problem becomes quite similar to that in the axisymmetric case.

In this paper, taking advantage of recent progress both in the definition of the circumference and in finding apparent horizons numerically, we study, for the first time, the condition for the formation of apparent horizons in the light of the hoop conjecture in spaces without axisymmetry but with a discrete symmetry. We present the momentarily static vacuum configurations. We consider two families of configurations as a demonstration: black holes distributed on a ring, and black holes on a spherical surface. We increase the number of black holes keeping the total mass constant and explore the existence of a common apparent horizon. As for the definition of a mass we simply adopt the ADM mass, because of its uniqueness and definiteness at least for the initial data on a spacelike hypersurface.

This paper is organized as follows. In Sec.2, first we review the method for finding apparent horizons in spaces with a discrete symmetry, and then we also review a definition of the circumference of a body which has been proposed by us, and finally we present the results of our numerical analysis of the initial data. Section 3 is devoted to summary.

II. INITIAL DATA ANALYSIS

A. Finding Apparent Horizons

A marginally trapped surface is a closed 2-surface S where the expansion Θ of future-directed outgoing null vectors ℓ^μ normal to it vanishes [7]. An apparent horizon is defined as the outer boundary of a connected component of the trapped region. When the apparent horizon forms, there always exists the event horizon enclosing it if there is no naked singularity and the null convergence condition is satisfied [7].

Let s^μ be the outward-pointing spacelike unit normal to S and n^μ be the unit normal to a time slice. Then ℓ^μ can be written as $\ell^\mu = n^\mu + s^\mu$ and thus

$$\Theta = D_i s^i + K_{ij} s^i s^j - K = 0 \quad (2.1)$$

on S .

In this paper, we consider the conformally flat space for simplicity

$$dl^2 = \psi^4 f_{ij} dx^i dx^j, \quad (2.2)$$

where f_{ij} denotes the flat metric. Then Eq.(2.1) is rewritten as

$$\begin{aligned} \Theta = & -\frac{r}{\psi^2(r^2 + r_\theta^2)^{3/2}} \left[r_{\theta\theta} + r_\theta \cot \theta + \frac{r_{\phi\phi}}{\sin^2 \theta} - 2r - \frac{3}{r} \left(r_\theta^2 + \frac{r_\phi^2}{\sin^2 \theta} \right) \right. \\ & - 4 \left(\frac{\psi_r}{\psi} - \frac{\psi_\theta}{\psi} \frac{r_\theta}{r^2} - \frac{\psi_\phi}{\psi} \frac{r_\theta}{r^2 \sin^2 \theta} \right) \left(r^2 + r_\theta^2 + \frac{r_\phi^2}{\sin^2 \theta} \right) + \frac{r_\theta^2}{r^2} \left(r_\theta \cot \theta + \frac{r_{\phi\phi}}{\sin^2 \theta} \right) \\ & \left. - 2 \frac{r_\theta r_\phi}{r^2 \sin^2 \theta} (r_{\theta\phi} - r_\phi \cot \theta) + \frac{r_{\theta\theta} r_\phi^2}{r^2 \sin^2 \theta} \right] + K_{ij} s^i s^j - K = 0, \end{aligned} \quad (2.3)$$

where $r(\theta, \phi)$ parameterizes the surface of the apparent horizon and $r_\theta \equiv \partial r / \partial \theta$. This is the elliptic partial differential equation about θ and ϕ . It is difficult in general to solve numerically Eq.(2.3) efficiently and robustly, and several methods have been proposed so far [8–11].

Since we are interested in the criterion of the formation of horizons, it is important to find horizons robustly. In axisymmetric spaces, Eq.(2.3) can be solved as a two-point boundary value problem [12]. And it is proved to be a robust method to find apparent horizons since the regularity of the apparent horizon on the symmetry axis is automatically guaranteed. It is desirable to solve Eq.(2.3) in a similar manner in the non-axisymmetric space. To do so, we assume that the space has a discrete symmetry such that $r(\theta, \phi + \pi) = r(\theta, \phi)$. We also assume the space has a reflection symmetry about $\theta = \pi/2$ plane. The latter assumption is just for simplicity and is not essential for the method. Then the axis $\theta = 0$ becomes the symmetry axis as in the axisymmetric case. Thus we can specify the boundary condition at $\theta = 0, \pi/2$ as

$$r_\theta = 0. \quad (2.4)$$

Hence we can solve Eq.(2.3) as a boundary value problem [10] although the space is not axisymmetric. By finite-differencing Eq.(2.3) with taking account of the discrete symmetry and the boundary condition Eq.(2.4), it becomes a matrix equation, and we solve it iteratively. The detailed numerical implementation of the method is given in [10]. When the apparent horizon forms, we compute its area A

$$A = 4 \int_0^\pi \int_0^{\pi/2} \psi^4 r^2 \sin \theta d\phi d\theta \sqrt{1 + \frac{r_\theta^2}{r^2} + \frac{r_\phi^2}{r^2 \sin^2 \theta}}. \quad (2.5)$$

In the numerical results shown below, we discretize θ and ϕ as follows

$$\theta_i = \left(i - \frac{1}{2}\right) \frac{\pi}{2N_\theta}, \quad \phi_j = \left(j - \frac{1}{2}\right) \frac{\pi}{N_\phi}, \quad (2.6)$$

with $i = 1, \dots, N_\theta$, and $j = 1, \dots, N_\phi$. We typically take the grid numbers $N_\theta = N_\phi = 64$ and sometimes $N_\theta = N_\phi = 128$ when a higher resolution is required.

B. Calculating Hoop

To gauge the hoop conjecture, we calculate the proper lengths of geodesics of various orientations that enclose the entire configuration. Due to the symmetry such that the reflection symmetry about the equatorial plane and the discrete symmetry about the $\theta = 0$ axis, the equatorial ($\theta = \pi/2$) plane and some $\phi = \text{constant}$ surfaces take the special position. The appropriate circumference should be the maximum of (i) the minimum equatorial circumference \mathcal{C}_{eq}^{min} and (ii) the minimum polar circumference along $\phi = \text{constant}$ plane \mathcal{C}_{pol}^{min} .

The geodesic equation on the equatorial plane is given by

$$r_{\phi\phi} = -2 \frac{\psi_\phi}{\psi} \frac{r_\phi^3}{r^2} + \left(2 \frac{\psi_r}{\psi} + \frac{2}{r}\right) r_\phi^2 - 2 \frac{\psi_\phi}{\psi} r_\phi + \left(2 \frac{\psi_\phi}{\psi} + \frac{1}{r}\right). \quad (2.7)$$

We note that \mathcal{C}_{eq}^{min} is well-defined only if the equatorial plane symmetry is assumed as in the recent 3D dynamical calculations on coalescing binary NSs/BHs [13]. On the other hand, geodesics along the $\phi = \text{constant}$ plane do not exist in general. However, if we restrict ourselves to the plane with the symmetry such that $\psi_\phi = 0$, then such geodesics do exist and follow the equation:

$$r_{\theta\theta} = -2 \frac{\psi_\theta}{\psi} \frac{r_\theta^3}{r^2} + \left(2 \frac{\psi_r}{\psi} + \frac{2}{r}\right) r_\theta^2 - 2 \frac{\psi_\theta}{\psi} r_\theta + \left(2 \frac{\psi_\theta}{\psi} + \frac{1}{r}\right). \quad (2.8)$$

Eq.(2.7) and Eq.(2.8) are the same except for the replacement $\phi \rightarrow \theta$, and we solve them by the fourth-order Runge-Kutta method. We vary r and $r_\phi(r_\theta)$ at $\phi = 0(\theta = 0)$ and compute \mathcal{C} encompassing all black holes using Eq.(2.7)(Eq.(2.8)) up to $\phi = \pi(\theta = \pi/2)$. In this way we obtain the minimum circumference:

$$\mathcal{C}_{eq}^{min} = 2 \int_0^\pi \psi^2 (r^2 + r_\phi^2)^{\frac{1}{2}} d\phi, \quad (2.9)$$

$$\mathcal{C}_{pol}^{min} = 4 \int_0^{\pi/2} \psi^2 (r^2 + r_\theta^2)^{\frac{1}{2}} d\theta. \quad (2.10)$$

We note that when we compute the minimum polar circumference, we first minimize the circumference with being ϕ fixed and then maximize over ϕ which satisfies $\psi_\phi = 0$.

C. Numerical Results

Now we construct the vacuum initial data. We consider the time-symmetric initial data, that is, $K_{ij} = 0$. Then the only constraint equation we have to solve is the Hamiltonian constraint equation

$$\Delta\psi = 0, \quad (2.11)$$

where Δ denotes the flat Laplacian. We consider the following configurations: (1) black holes distributed on a ring, (2) black holes on a spherical surface.

1. Case (1)

We show the numerical results for the case (1): black holes distributed on a ring.

We consider N black holes (where N is an even number) of an equal mass distributed on a ring of radius a such that each black hole's Cartesian coordinate is $(a \cos(2\pi l/N), a \sin(2\pi l/N), 0)$, where $l = 0, \dots, N-1$. Then the solution of the constraint Eq.(2.11) is

$$\psi(r, \theta, \phi) = 1 + \frac{M}{2N} \sum_{l=0}^{N-1} \frac{1}{\sqrt{r^2 - 2ar \sin \theta \cos(\phi - 2\pi l/N) + a^2}}, \quad (2.12)$$

where M is the ADM mass of the total system. In the limit of large N the configuration becomes the singular ring, and the solution becomes

$$\psi(r, \theta) = 1 + \frac{M}{\pi \sqrt{r^2 + 2ar \sin \theta + a^2}} K(\kappa), \quad (2.13)$$

where $K(\kappa)$ is the elliptic integral of the first kind with

$$\kappa^2 = \frac{4ar \sin \theta}{r^2 + 2ar \sin \theta + a^2}. \quad (2.14)$$

The results are shown in Fig.1 and Table 1. The top view of the apparent horizon as well as the bird's-eye view of it is shown. The shape of the apparent horizon indeed respects the discrete symmetry of the configuration. As N increases, the shape becomes pancake-like. The maximum of $(\mathcal{C}_{eq}^{min}, \mathcal{C}_{pol}^{min})$ is shown in the table. We calculate the circumference \mathcal{C} of the system irrespective of the existence of an apparent horizon. Even if the apparent horizon forms, the appropriate circumference is generally not located on it. The circumference on the apparent horizon can be significantly larger [2,6,14].

When the apparent horizon forms, its area A normalized by $16\pi M^2$ is computed because in the time-symmetric initial data the following inequality holds if the final state is stationary:

$$A \leq A_{EH} \leq A_f (= 16\pi M_f^2) \leq 16\pi M^2. \quad (2.15)$$

Here A_{EH} is the area of the event horizon. We note that the existence of an apparent horizon implies the existence of the event horizon enclosing it [7]. From this and the fact that the

apparent horizon is the minimum surface in the time-symmetric initial data [15], the first inequality holds. A_f is the final stationary state black hole's area, and the second inequality follows from the area theorem [7]. From the uniqueness theorem [16], the final state is the Schwarzschild black hole with mass M_f because we are considering the non-rotating system. M_f should not be larger than the initial mass M because gravitational radiation conveys the energy during the dynamical evolution.

In the cases $N = 2$ and $N \rightarrow \infty$, we also show the numerical results using a 2D(axisymmetric) apparent horizon finder [12] for comparison and the check of our numerical results. We find good agreement.

2. Case (2)

Next we show the numerical results for the case (2): black holes on a spherical surface.

Black holes are distributed on a sphere of radius a such that each black hole's Cartesian coordinate is

$$(a \sin(\pi k/n) \cos(2\pi l/n), a \sin(\pi k/n) \sin(2\pi l/n), a \cos(\pi k/n)), \quad (2.16)$$

where $k = 1, \dots, n-1, l = 0, \dots, n-1$. We also consider two additional black holes located at $\theta = 0$, and π on the surface so that in the large N limit the configuration becomes a singular spherical surface. The total number of black holes is then $N = n(n-1) + 2$. We assume n is even number. The solution of the constraint Eq.(2.11) is simply

$$\begin{aligned} \psi(r, \theta, \phi) = 1 + \frac{M}{2N} & \left(\frac{1}{\sqrt{r^2 + 2ar \cos \theta + a^2}} + \frac{1}{\sqrt{r^2 - 2ar \cos \theta + a^2}} \right) \\ & + \frac{M}{2N} \sum_{k=1}^{n-1} \sum_{l=0}^{n-1} \frac{1}{\sqrt{r^2 + a^2 - 2ar (\sin \theta \sin(\pi k/n) \cos(\phi - 2\pi l/n) + \cos \theta \cos(\pi k/n))}}. \end{aligned} \quad (2.17)$$

The results are shown in Fig.2 and Table 2. For smaller N the apparent horizon is bumpy. Since the system becomes spherically symmetric in the large N limit, $A/16\pi M^2$ becomes close to 1 as N increases and \mathcal{C} does not clearly distinguish the existence or non-existence of the apparent horizon.

III. SUMMARY

We tested the hoop conjecture in spaces without axisymmetry but with a discrete symmetry. The existence or nonexistence of an apparent horizon encompassing all black holes is qualitatively consistent with the hoop conjecture proposed by Thorne. From Table 1 and Table 2, we find that if the circumference \mathcal{C} satisfies $\mathcal{C}/4\pi M \lesssim 1.168$, then the configuration will be surrounded by a common apparent horizon.

In non-axisymmetric spaces with a discrete symmetry, searching for hoops is less computationally demanding than searching for apparent horizons: just solving the ordinary differential equation. Further if the equatorial plane symmetry is assumed as in the recent 3D dynamical calculations on coalescing binary NSs/BHs [13], \mathcal{C}_{eq}^{min} is then well-defined, and therefore even in more general spaces the hoop concept can be a useful diagnostic for the final fate of the collapsed object.

ACKNOWLEDGMENTS

The author would like to thank Professor T.Nakamura for encouragement and Professor N.Sugiyama for a careful reading of the manuscript. He is also grateful to an anonymous referee for useful comments which improved the manuscript. This work was supported in part by YITP and in part by a JSPS Fellowship for Young Scientists under grant No.3596.

REFERENCES

- [1] K. S. Thorne, in *Magic without Magic*: John Archibald Wheeler, edited by J.Klauder (Freeman, San Francisco, 1972).
- [2] T. Nakamura, S. T. Shapiro, and S. A. Teukolsky, Phys. Rev. **D38**, 2972 (1988).
- [3] E. Flanagan, Phys. Rev. **D44**, 2409 (1991).
- [4] S. T. Shapiro and S. A. Teukolsky, Phys. Rev. Lett. **66**, 994 (1991); Phys. Rev. **D45**, 2206 (1992).
- [5] A. M. Abrahams, K. R. Heiderich, S. L. Shapiro, S. A. Teukolsky, Phys. Rev. **D46**, 2452 (1992).
- [6] T. Chiba, T. Nakamura, K. Nakao, and M. Sasaki, Class.Quantum Grav. **11**, 431 (1994).
- [7] S. W. Hawking and G. F. R. Ellis, *The Large Scale Structure of Space-Time*, (Cambridge University Press, 1973).
- [8] T. Nakamura, Y. Kojima, and K. Oohara, Phys. Lett. **A106**, 235 (1984); *ibid* **A107**, 452 (1985).
- [9] T. W. Baumgarte, G. B. Cook, M. A. Scheel, S. L. Shapiro, S. A. Teukolsky, Phys.Rev. **D54**, 4849 (1996); P. Anninos, K. Camarda, J. Libson, J. Massó, E. Seidel, W.-M. Suen, Phys. Rev. **D58**, 024003(1998).
- [10] M. Shibata, Phys. Rev. **D55**, 2002 (1997).
- [11] C. Gundlach, Phys. Rev. **D57**, 863 (1998).
- [12] M. Sasaki, K. Maeda, S. Miyama, and T. Nakamura, Prog. Theor. Phys. **63**, 1051 (1980); T. Nakamura, K. Oohara, and Y. Kojima, Prog. Theor. Phys. Suppl. **90**, 1 (1987).
- [13] T. Nakamura, in *Relativistic Cosmology, the Proceedings of the 8th Nishinomiya-Yukawa Memorial Symposium*, edited by M.Sasaki (Universal Academy Press, Tokyo, 1994); P. Anninos et al., Phys.Rev. **D52**, 2059 (1995).
- [14] S. Brandt and E. Seidel, Phys. Rev. **D54**, 1403 (1996).
- [15] G. W. Gibbons, Commun. Math. Phys. **27**, 87 (1972).
- [16] W. Israel, Phys. Rev. **164**, 1776 (1967).

FIGURE CAPTION

Fig.1. The shape of the apparent horizon for the case (1) near the critical separation is shown for (a) $N = 2$, (b) $N = 4$, (d) $N = 6$, (d) $N = 10$ and (e) $N = \infty$. The top view of the apparent horizon as well as the bird's-eye view of it is shown. As N increase the shape becomes pancake-like. The coordinates are in units of M .

Fig.2. The shape of the apparent horizon for the case (2) near the critical separation is shown for (a) $N = 4$, (b) $N = 14$, (c) $N = 32$ and (d) $N = 58$. For smaller N the surface is bumpy. As N increases it becomes spherical.

TABLE CAPTION

Table 1. Properties of black holes distributed on a ring. Here “2D” indicates the numerical results using an axisymmetric apparent horizon finder. “Y” means that apparent horizon enclosing all black holes are found; “N” means the opposite. $\mathcal{C} = \max(\mathcal{C}_{eq}^{min}, \mathcal{C}_{pol}^{min})$.

Table 2. Properties of black holes on a spherical surface.

Table 1a: N=2 case

a/M	AH?	$\mathcal{C}/4\pi M$	$A/16\pi M^2$	$A/16\pi M^2(2D)$
0.38	Y	1.114	0.9780	0.9780
0.383	Y	1.115	0.9769	0.9769
0.39	N	1.118		

Table 1b: N=4 case

a/M	AH?	$\mathcal{C}/4\pi M$	$A/16\pi M^2$
0.41	Y	1.140	0.9865
0.42	Y	1.144	0.9841
0.43	N	1.149	

Table 1c: N=6 case

a/M	AH?	$\mathcal{C}/4\pi M$	$A/16\pi M^2$
0.43	Y	1.154	0.9883
0.44	Y	1.159	0.9860
0.45	N	1.163	

Table 1d: N=10 case

a/M	AH?	$\mathcal{C}/4\pi M$	$A/16\pi M^2$
0.45	Y	1.163	0.9875
0.46	Y	1.168	0.9857
0.47	N	1.173	

Table 1e: N= ∞ (ring) case

a/M	AH?	$\mathcal{C}/4\pi M$	$A/16\pi M^2$	$A/16\pi M^2(2D)$
0.49	Y	1.155	0.9817	0.9812
0.495	Y	1.158	0.9794	0.9797
0.505	N	1.163		

Table 2a: N=4 case

a/M	AH?	$\mathcal{C}/4\pi M$	$A/16\pi M^2$
0.40	Y	1.136	0.9890
0.41	Y	1.140	0.9870
0.42	N	1.145	

Table 2b: N=14 case

a/M	AH?	$\mathcal{C}/4\pi M$	$A/16\pi M^2$
0.40	Y	1.068	0.9982
0.43	Y	1.076	0.9965
0.44	Y	1.079	0.9954
0.45	N	1.082	

Table 2c: N=32 case

a/M	AH?	$\mathcal{C}/4\pi M$	$A/16\pi M^2$
0.40	Y	1.054	0.9992
0.44	Y	1.062	0.9982
0.45	Y	1.064	0.9975
0.46	N	1.066	

Table 2d: N=58 case

a/M	AH?	$\mathcal{C}/4\pi M$	$A/16\pi M^2$
0.40	Y	1.051	0.9993
0.44	Y	1.058	0.9986
0.45	Y	1.060	0.9983
0.46	N	1.061	

FIGURES

Fig 1(a) (continued)

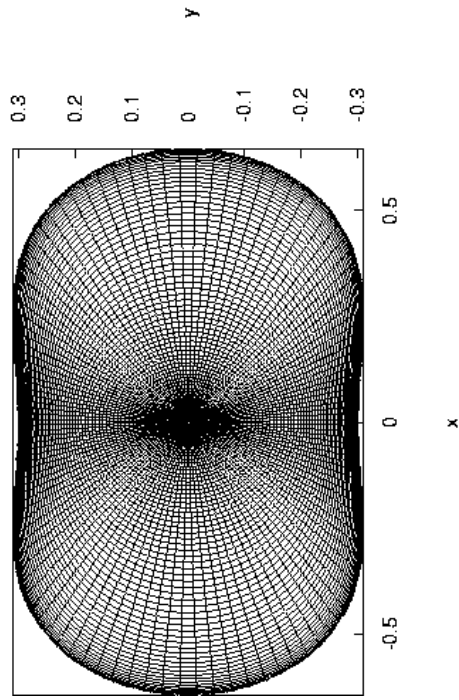
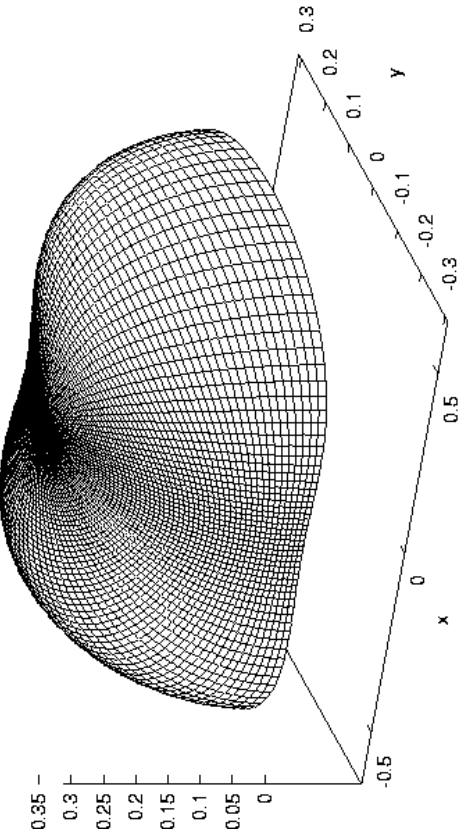


Fig 1(a)



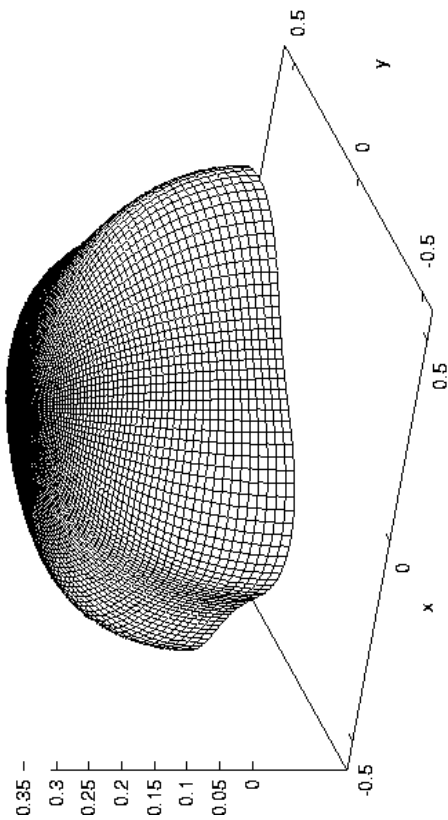


Fig 1(b)

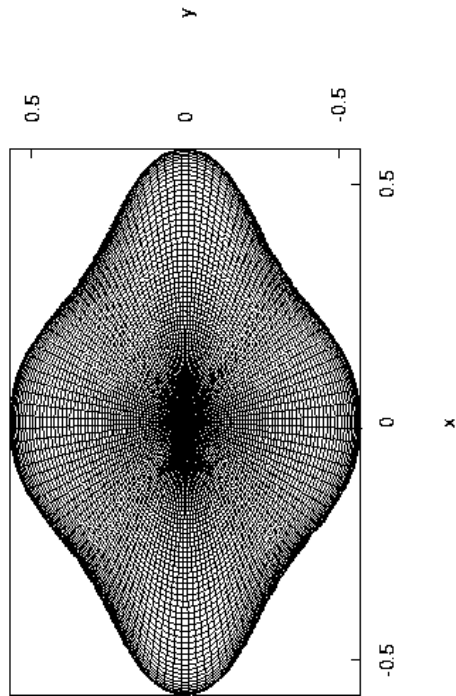


Fig 1(b) (continued)

Fig. 1(c)

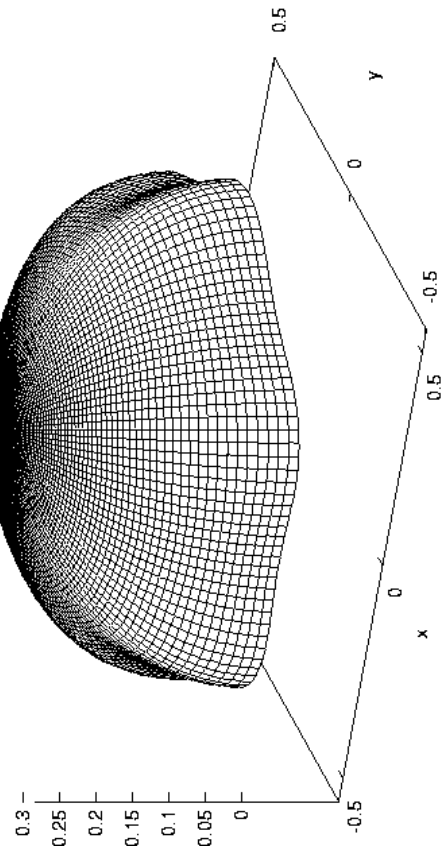


Fig. 1(c) (continued)

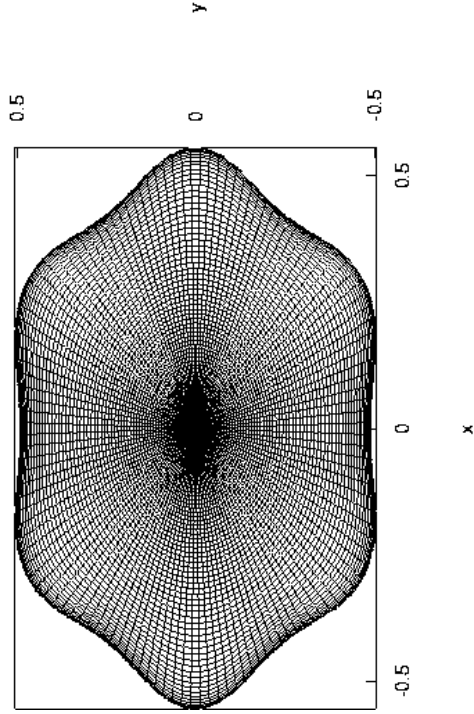


Fig 1(d)

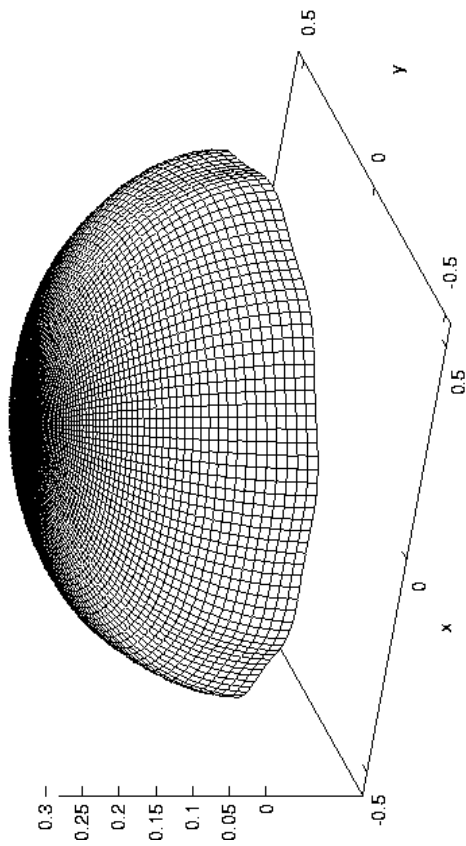


Fig 1(d) (continued)

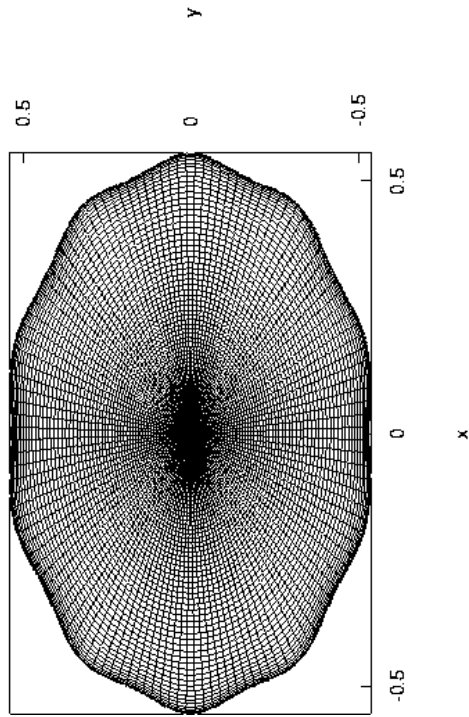


Fig 1(e)

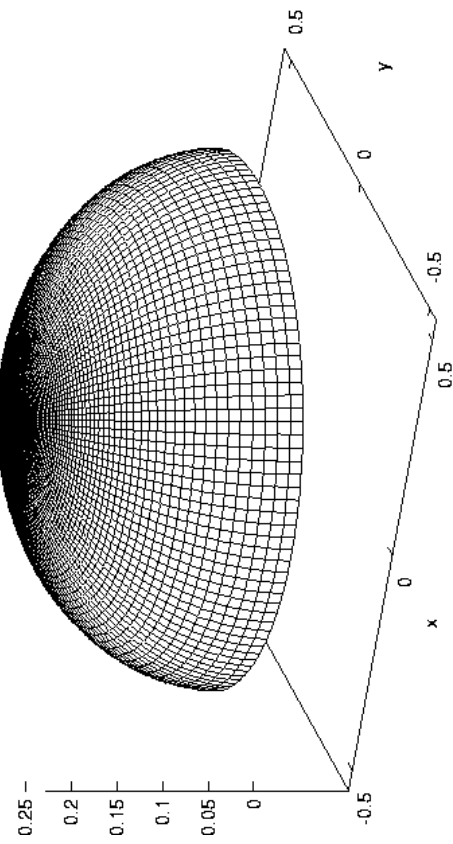


Fig 1(e) (continued)

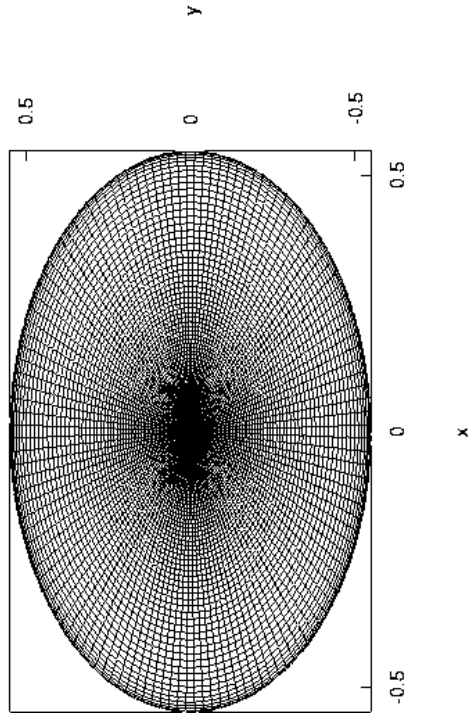


Fig.2(a)

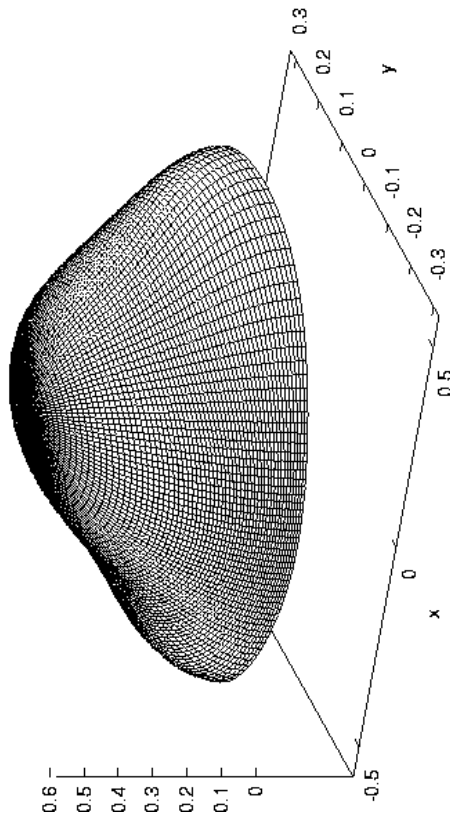


Fig.2(b)

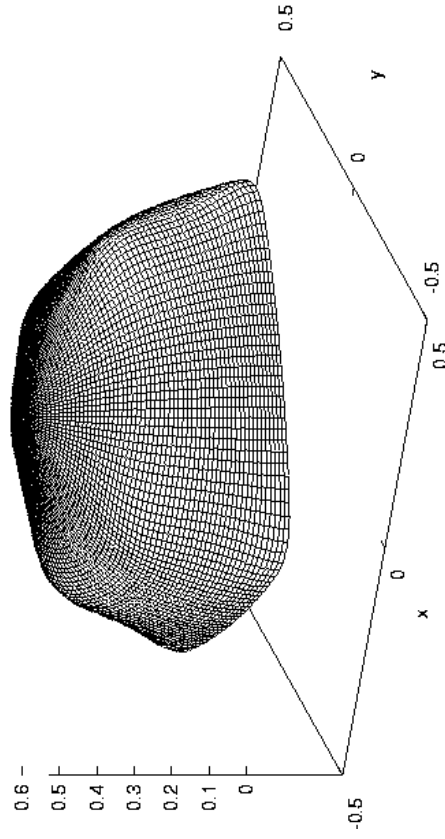


Fig.2(c)

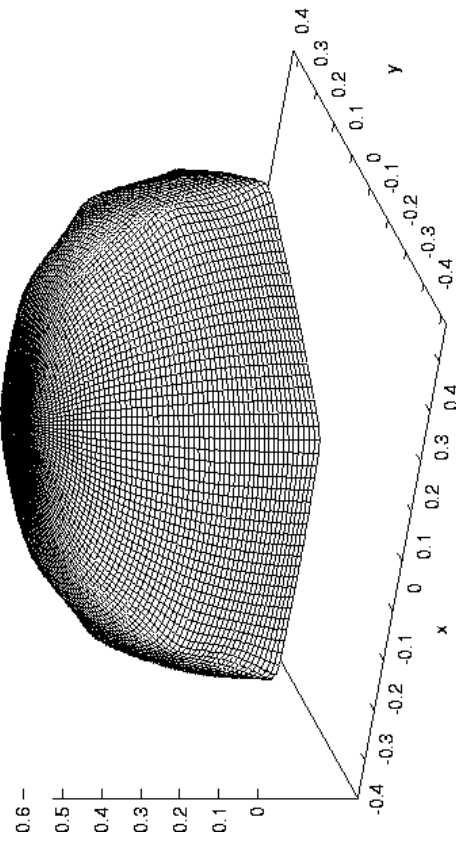


Fig.2(d)

